Electronic Supplementary Material (ESI) for Materials Horizons.

Supporting information

High defect tolerance β-$CsSnI_3$ perovskite light-emitting diodes

Haixuan Yu [1#], Tao Zhang [1#], Zhiguo Zhang [1], Zhirong Liu [1], Qiang Sun [1], Junyi Huang [1], Letian Dai[1], Yan Shen [1], Xiongjie Li [1]*, Mingkui Wang [1, 2]*

Experimental Section

Materials: PEDOT:PSS (aqueous dispersion, 4083) was purchased from Xi'an Polymer Light Technology Corp, B3PYMPM (99%) was purchased from Jilin Optical and Electronic Materials Co. Ltd., Cesium iodide (CsI, 99.9%), Cesium formate (CsFa, 98%), Tin iodide (SnI_2, 99.99%), Tin fluoride (SnF_2, 99.99%), N,N-dimethylformamide (DMF) (anhydrous, 99.8%), chlorobenzene (anhydrous, 99.8%), dimethyl sulfoxide (DMSO) (anhydrous, 99.9%), were purchased from Sigma-Aldrich. All the materials were used as received without further purification.

Perovskite Films Fabrication: The 0.2 M perovskite precursor solution was prepared by dissolving CsI, SnI_2, SnF_2, and CsFa at the molar ratio of 1:1:0.1: X (X=1 to 4 %) in mixed solvent (DMF: DMSO = 4:1) and stirring at 25 °C for 4 h. The perovskite precursor solution was filtered by a 0.22 μm PTFE filter before depositing. The precursor solution was deposited onto the substrate via the spin coating process at 3000 rpm for 30 s. Immediately, the substrate was annealed at 110 °C for 10 min. All the processes were carried out in a nitrogen-filled glove box.

Devices Fabrication: The glass substrates were cleaned by sonicating in deionized water, isopropyl alcohol and then dried by nitrogen flow, followed by ultraviolet-ozone treatment for 10 min. The PEDOT:PSS layer was spin-coated on the substrates at 4000 rpm for 40 s followed by annealed in air at 150 °C for 15 min. After the deposition of perovskite films, B3PyMPM (50 nm), and LiF/Al electrodes (1 nm/100 nm) were deposited in a thermal evaporator at a pressure of ~6×10^{-6} Torr. The device area was 7.25 mm^{-2}.

DFT calculations: The electronic structure of $CsSnI_3$ was calculated by density functional theory (DFT) using the CASTEP program code with the plane-wave pseudopotential method. We adopted the generalized gradient approximation (GGA) in the form of the Perdew−Burke−Ernzerhof (PBE) for the exchange-correlation potentials. The ultrasoft scalar relativistic pseudopotential was used with a plane-wave energy cutoff of 300 eV. The first Brillouin zone was sampled with grid spacing of 0.037 $Å^{-1}$. The self-consistent field was used with a tolerance of 5×10^{-7} eV/atom. To improve the accuracy of the bandgap which is usually underestimated within the GGA,

the Heyd-Scuseria-Ernzerhof (HSE) hybrid functional was adopted including spin−orbit coupling (SOC) using the PWmat code with the NCPP-SG15-PBE-SOC pseudopotential. The lattice constants and atomic coordinates used in the calculations were derived from the experimental results.

Characterization

PeLED characterizations: PeLED device characterizations were performed at room temperature in a nitrogen-filled glovebox without encapsulation. A Keithley 2400 source-meter and a fibre integration sphere (FOIS-1) coupled with a QE Pro spectrometer (Ocean Optics) were utilized. The absolute radiance was calibrated by a standard Vis–NIR light source (HL-3P-INT-CAL plus, Ocean Optics). The PeLED devices were measured on top of the integration sphere and only forward light emission can be collected. The devices were swept from zero bias to forward bias with a step voltage of 0.05 V, lasting for 100 ms at each voltage step for stabilisation. The sweep duration from 1 to 7 V is 70 sec (with a scan rate of 86 mV S^{-1}). The EQE and spectral evolution with time was measured using the same system.

Materials characterizations: The X-ray diffraction patterns were carried out using Cu Kα radiation source (XRD, Shimadzu XRD-6100 diffractometer). Steady-state PL spectra and temperature-dependent PL were performed using a fluorescence spectrophotometer (LabRAM HR800) with an excitation wavelength of 532 nm. UV-vis absorption spectra were observed with a PE950 spectrophotometer. FTIR was tested on a Bruker VERTEX 70. Time-resolved PL decays were measured by a Delta Flex Fluorescence Lifetime System (Horiba Scientific Com., Japan). The PLQY of the 2D perovskite films was characterized by a three-step technique with a 532 nm CW laser and spectrometer in an integrating sphere. U Surface morphology was observed by a field emission SEM (Nova NanoSEM 450).

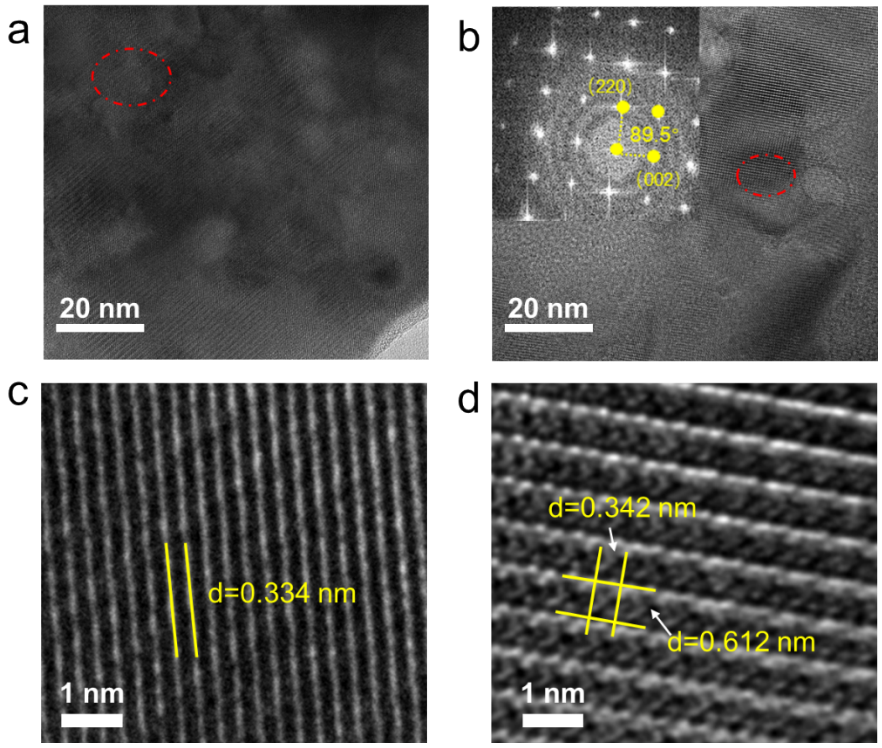

Figure S1. TEM and HR-TEM images of the $CsSnI_3$ without (a, c) and with (b, d) CsFa treatment and corresponding FFT pattern (inset).

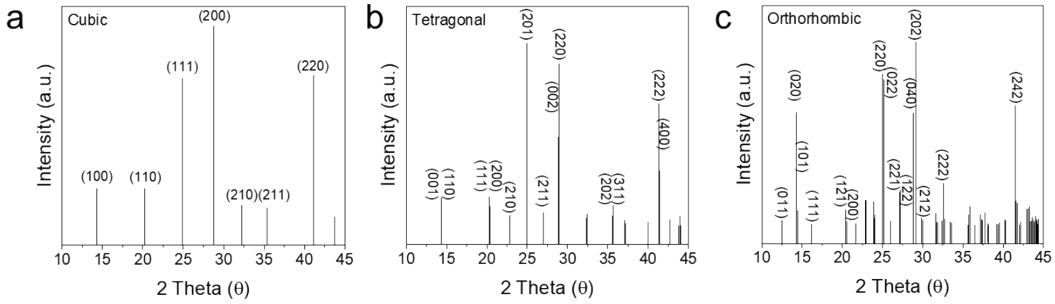

Figure S2. Comparison of standard XRD patterns of (a) α-$CsSnI_3$, (b) β-$CsSnI_3$ and (c) γ-$CsSnI_3$.

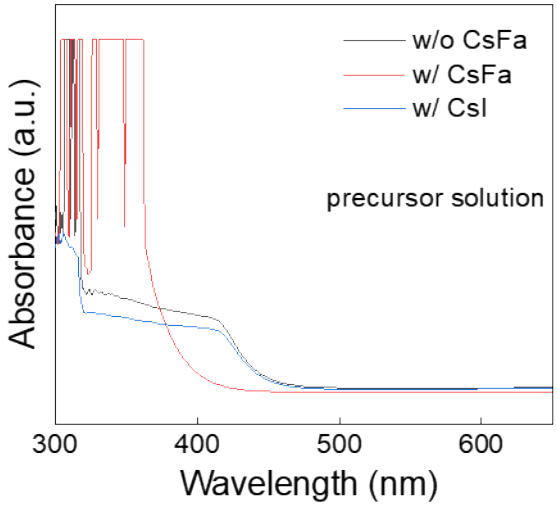

Figure S3. UV-vis absorption for different precursor solutions.

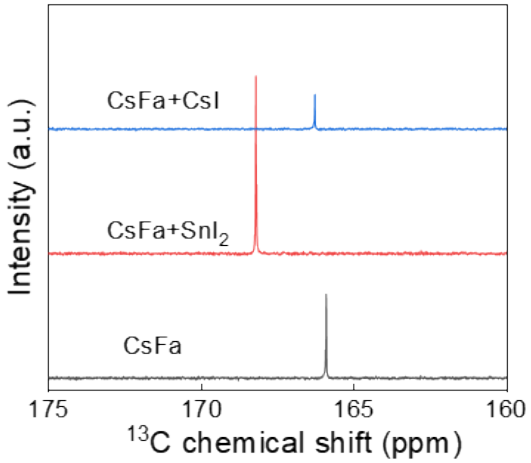

Figure S4. ^{13}C NMR spectra of CsFa, CsFa+SnI_2, and CsFa+CsI in the DMSO-d_6 solvent.

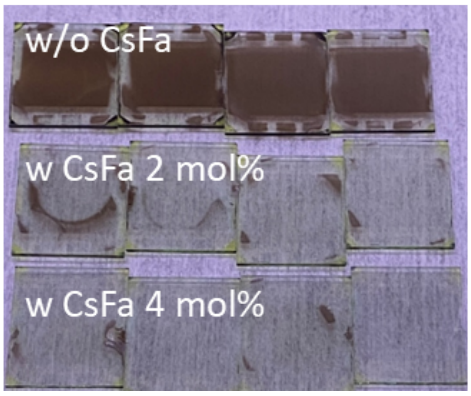

Figure S5. Color change of pre-annealing $CsSnI_3$ films after 30 min of storing in glovebox.

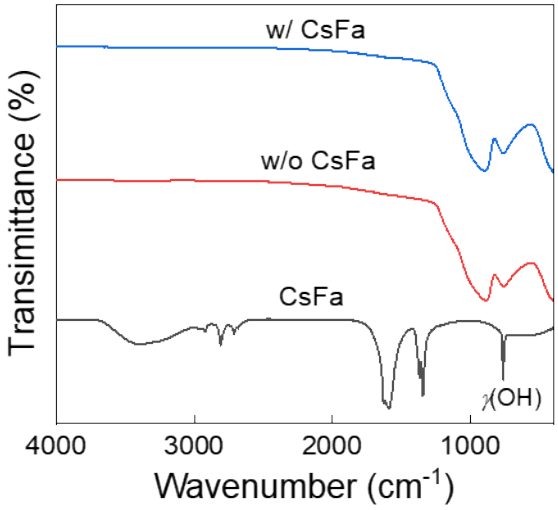

Figure S6. FTIR spectra of cesium formate (CsFa), $CsSnI_3$, and CsFa-treated $CsSnI_3$ film.

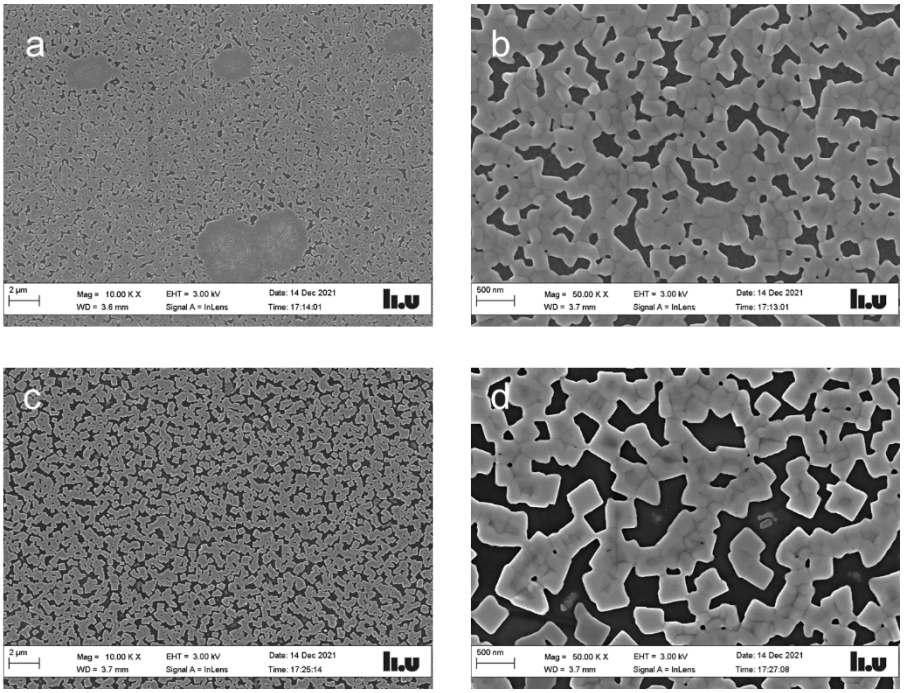

Figure S7. SEM images of $CsSnI_3$ perovskite films (a-b) without and (c-d) CsFa treatment.

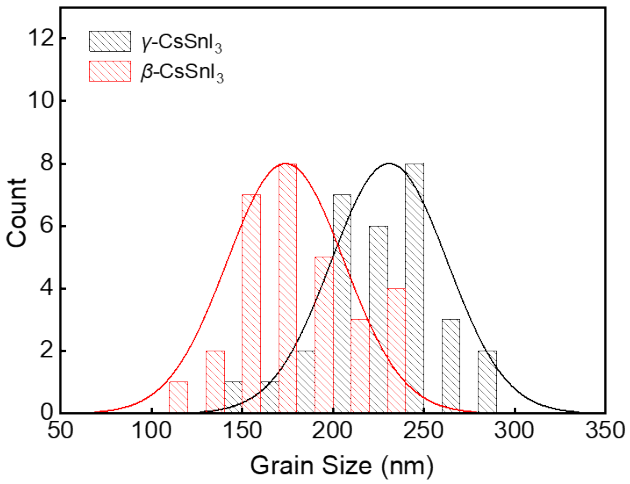

Figure S8. Grain size distribution of $CsSnI_3$ perovskite films without and with CsFa treatment.

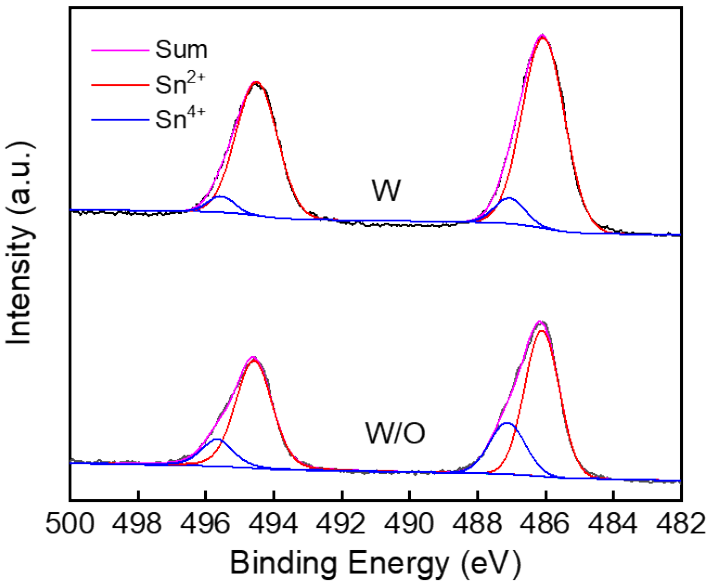

Figure S9. XPS spectra of $CsSnI_3$ perovskite films without and with CsFa treatment.

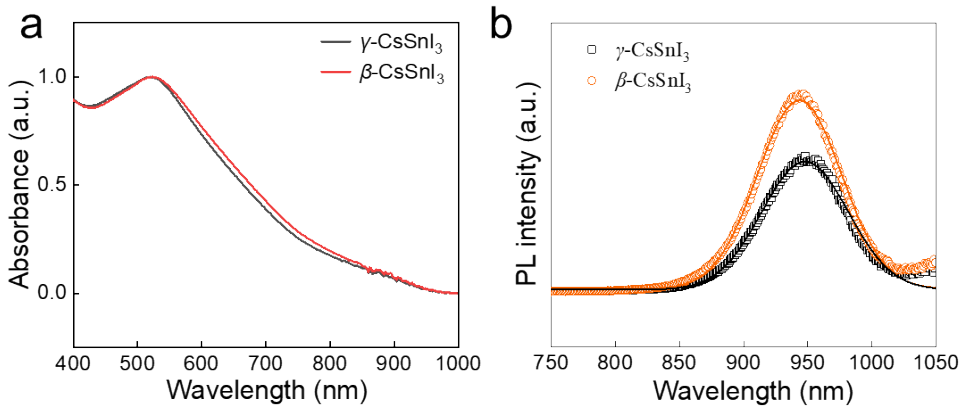

Figure S10. (a) Absorption spectra and (b) steady-state PL of γ-$CsSnI_3$ and β-$CsSnI_3$ films.

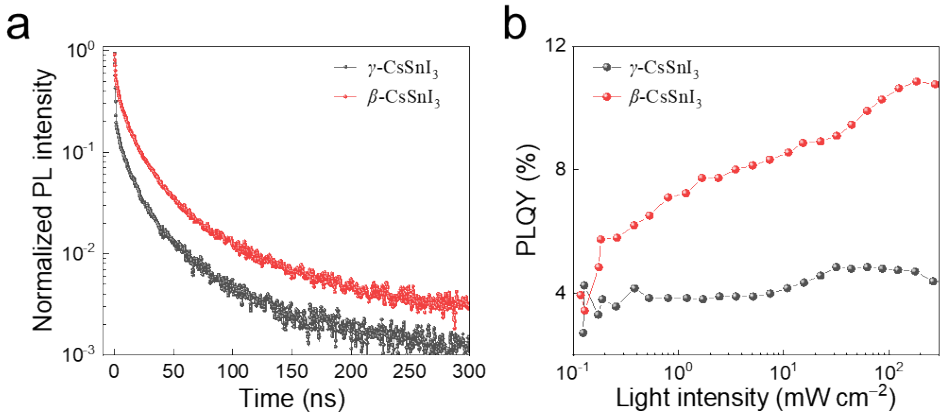

Figure S11. (a) Time-resolved photoluminescence decay curves of different $CsSnI_3$ films and (b) excitation-intensity-dependent PLQY.

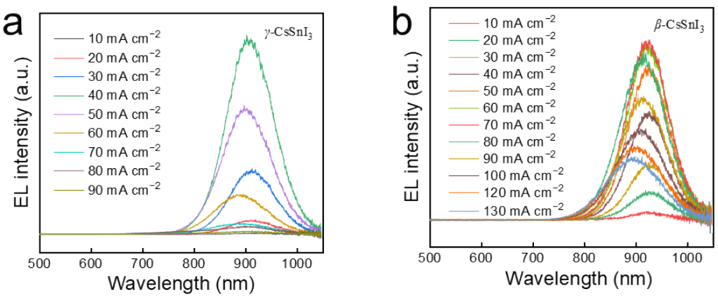

Figure S12. Current density dependent electroluminescence spectra of PeLEDs based on γ-$CsSnI_3$ (a) and β-$CsSnI_3$ (b) films.

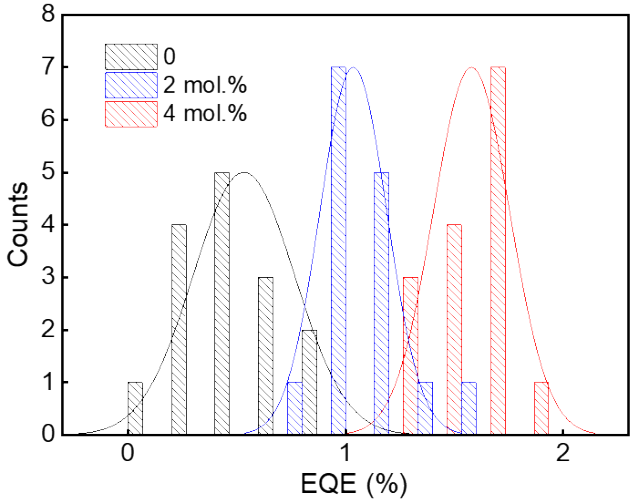

Figure S13. Statistical EQEs of the Pero-LEDs based on the $CsSnI_3$ with different concentrations of CsFa.

Table S1. A summary of experimental and theoretical values for the lattice spacings of two planes and the angle between them of β-$CsSnI_3$ sample.

	$d_{(220)}$	$d_{(002)}$	φ
Theoretical values	3.49 Å	6.18 Å	90.0°
Experimental values	3.42 Å	6.12 Å	89.5°

Table S2. A summary of the main characteristics of the reported tin-based perovskite light-emitting diodes in recent years.

No.	Materials	Structures	PLQY(%)	EQE (%)	Lifetime	Measurement conditions	Ref.
1	γ-$CsSnI_3$	ITO/ PEDOT:PSS/Perovskite/B3PyMPM/LiF/Al	-	5.4	23.6 h	J = 100 mA.cm^{-2}	[1]
2	γ-$CsSnI_3$	ITO/PEDOT:PSS/ Perovskite /TPBi/LiF/Al	-	~3.2	39.5 h	J =100 mA.cm^{-2}	[2]
3	γ-$CsSnI_3$	ITO/PEDOT:PSS/ perovskite /LiF/Al	-	0.01	-	-	[3]
4	γ-$CsSnI_3$	ITO/PEDOT:PSS/ perovskite/PBD/LiF/Al		0.02	-	-	[4]
5	$CH_3NH_3Sn(Br_{1-x}I_x)_3$	ITO/PEDOT:PSS/ Perovskite /F8/Ca/Ag	5.3	0.72	-	-	[5]
6	PEA_2SnI_4	ITO/PEDOT:PSS/ Perovskite /TPBi/LiF/Al	-	0.361%	-	-	[6]
7	TEA_2SnI_4	ITO/PEDOT:PSS/ perovskite/TPBi/LiF/Al	1.52	0.62	25 S	J = 25 mA.cm^{-2}	[7]
8	β-$CsSnI_3$	ITO/ PEDOT:PSS/ Perovskite /B3PyMPM/LiF/Al	10	1.81	8.5 h 6 min	J = 100 mA.cm^{-2} J = 1000 mA.cm^{-2}	This work

References

[1] J. Lu, X. Guan, Y. Li, K. Lin, W. Feng, Y. Zhao, C. Yan, M. Li, Y. Shen, X. Qin, Z. Wei, *Adv. Mater.* 2021, **33**, 2104414.

[2] F. Yuan, G. Folpini, T. Liu, U. Singh, A. Treglia, J. Lim, J. Klarbring, S. Simak, I. Abrikosov, T. Sum, A. Petrozza, F. Gao, *Nat. Photon.* 2024, **18**, 170–176.

[3] K. Mahesh, C. Chang, W. Hong, T. Wen, P. Lo, H. Chiu, C. Hsu, S. Horng, Y. Chao, *RSC Adv.* 2020,**10**, 37161-37167.

[4] W. Hong, P. Lo, H. Chiu, S. Horng, Y. Chao, *Adv. Mater. Interfaces*, 2021, **8**, 2002240.

[5] M. Lai, T. Tay, A. Sadhanala, S. Dutton, G. Li, R. Friend, Z. Tan, *J. Phys. Chem. Lett.*, 2016, **7**, 2653-2658.

[6] Y. Heo, H. Jang, J. Lee, S. Jo, S. Kim, D. Ho, S. Kwon, K. Kim, I. Jeon, J. Myoung, J. Lee, J. Lee, J. Cho, *Adv. Funct. Mater.*, 2021, **31**, 2106974.

[7] Z. Wang, F. Wang, B. Zhao, S. Qu, T. Hayat, A. Alsaedi, L. Sui, K. Yuan, J. Zhang, Z. Wei, Z. Tan, *J. Phys. Chem. Lett.*, 2020, **11**, 1120-1127.